Brillouin optical correlation domain analysis with 4 millimeter resolution based on amplified spontaneous emission

Raphael Cohen, Yosef London, Yair Antman, and Avi Zadok*

Faculty of Engineering, Bar-Ilan University, Ramat-Gan 52900, Israel
Avinoam.Zadok@biu.ac.il

Abstract: A new technique for Brillouin scattering-based, distributed fiber-optic measurements of temperature and strain is proposed, analyzed, simulated, and demonstrated. Broadband Brillouin pump and signal waves are drawn from the filtered amplified spontaneous emission of an erbium-doped fiber amplifier, providing high spatial resolution. The reconstruction of the position-dependent Brillouin gain spectra along 5 cm of a silica single-mode fiber under test, with a spatial resolution of 4 mm, is experimentally demonstrated using a 25 GHz-wide amplified spontaneous emission source. A 4 mm-long localized hot spot is identified by the measurements. The uncertainty in the reconstruction of the local Brillouin frequency shift is ± 1.5 MHz. The single correlation peak between the pump and signal is scanned along a fiber under test using a mechanical variable delay line. The analysis of the expected spatial resolution and the measurement signal-to-noise ratio is provided. The measurement principle is supported by numerical simulations of the stimulated acoustic field as a function of position and time. Unlike most other Brillouin optical correlation domain analysis configurations, the proposed scheme is not restricted by the bandwidth of available electro-optic modulators, microwave synthesizers, or pattern generators. Resolution is scalable to less than one millimeter in highly nonlinear media.

©2014 Optical Society of America

OCIS codes: (290.5900) Scattering, stimulated Brillouin; (060.2370) Fiber optics sensors; (190.2055) Dynamic gratings; (190.4370) Nonlinear optics, fibers.

References and links

1. R. W. Boyd, *Nonlinear Optics*, 3rd ed. (Academic, 2008).
2. T. Kurashima, T. Horiguchi, and M. Tateda, "Distributed-temperature sensing using stimulated Brillouin scattering in optical silica fibers," Opt. Lett. **15**(18), 1038–1040 (1990).
3. T. Horiguchi, T. Kurashima, and M. Tateda, "A technique to measure distributed strain in optical fibers," IEEE Photon. Technol. Lett. **2**(5), 352–354 (1990).
4. M. Niklès, L. Thévenaz, and P. A. Robert, "Simple distributed fiber sensor based on Brillouin gain spectrum analysis," Opt. Lett. **21**(10), 758–760 (1996).
5. S. Martin-Lopez, M. Alcon-Camas, F. Rodriguez, P. Corredera, J. D. Ania-Castañon, L. Thévenaz, and M. Gonzalez-Herraez, "Brillouin optical time-domain analysis assisted by second-order Raman amplification," Opt. Express **18**(18), 18769–18778 (2010).
6. Y. Dong, L. Chen, and X. Bao, "Time-division multiplexing-based BOTDA over 100 km sensing length," Opt. Lett. **36**(2), 277–279 (2011).
7. Y. Peled, A. Motil, and M. Tur, "Fast Brillouin optical time domain analysis for dynamic sensing," Opt. Express **20**(8), 8584–8591 (2012).
8. A. Fellay, L. Thevenaz, M. Facchini, M. Nikles, and P. Robert, "Distributed sensing using stimulated Brillouin scattering: towards ultimate resolution.," in 12th International Conference on Optical Fiber Sensors, **Vol.** 16 of 1997 OSA Technical Digest Series (Optical Society of America, 1997), paper OWD3.
9. X. Bao and L. A. Chen, "Recent progress in Brillouin scattering based fiber sensors," Sensors (Basel) **11**(12), 4152–4187 (2011).

#206802 - $15.00 USD Received 19 Feb 2014; revised 28 Mar 2014; accepted 28 Mar 2014; published 12 May 2014
(C) 2014 OSA

10. Y. Dong, H. Zhang, L. Chen, and X. Bao, "2 cm spatial-resolution and 2 km range Brillouin optical fiber sensor using a transient differential pulse pair," Appl. Opt. **51**(9), 1229–1235 (2012).
11. Y. Antman, N. Primerov, J. Sancho, L. Thevenaz, and A. Zadok, "Localized and stationary dynamic gratings via stimulated Brillouin scattering with phase modulated pumps," Opt. Express **20**(7), 7807–7821 (2012).
12. Y. Antman, L. Yaron, T. Langer, M. Tur, N. Levanon, and A. Zadok, "Experimental demonstration of localized Brillouin gratings with low off-peak reflectivity established by perfect Golomb codes," Opt. Lett. **38**(22), 4701–4704 (2013).
13. K. Hotate and T. Hasegawa, "Measurement of Brillouin gain spectrum distribution along an optical fiber using a correlation-based technique-proposal, experiment and simulation," IEICE Trans. Electron. **E83-C**(3), 405–412 (2000).
14. K. Hotate, "Fiber distributed Brillouin sensing with optical correlation domain techniques," Opt. Fiber Technol. **19**(6), 700–719 (2013).
15. K. Y. Song, Z. He, and K. Hotate, "Distributed strain measurement with millimeter-order spatial resolution based on Brillouin optical correlation domain analysis," Opt. Lett. **31**(17), 2526–2528 (2006).
16. A. Zadok, Y. Antman, N. Primrov, A. Denisov, J. Sancho, and L. Thevenaz, "Random-access distributed fiber sensing," Laser Photon. Rev. **6**(5), L1–L5 (2012).
17. A. Denisov, M. A. Soto, and L. Thévenaz, "Time gated phase-correlation distributed Brillouin fiber sensor," Proc. SPIE **8794**, Fifth European Workshop on Optical Fibre Sensors, 87943I (2013).
18. D. Elooz, Y. Antman, N. Levanon, and A. Zadok, "High-resolution long-reach distributed Brillouin sensing based on combined time-domain and correlation-domain analysis," Opt. Express **22**(6), 6453–6463 (2014).
19. K. Hotate, H. Arai, and K. Y. Song, "Range-enlargement of simplified Brillouin optical correlation domain analysis based on a temporal gating scheme," SICE Journal of Control, Measurement, and System Integration **1**(4), 271–274 (2008).
20. J. W. Goodman, *Statistical Optics*, Wiley Classics Library Edition (John Wiley & Sons, 2000).
21. R. Cohen, Y. London, Y. Antman, and A. Zadok, "Few millimeter-resolution Brillouin optical correlation domain analysis using amplified-spontaneous-emission pump and signal waves," accepted for presentation in Optical Fiber Sensors Conference (OFS-23), Santander, Spain, June 2014. Proc. SPIE (2014).
22. K. Hotate, R. Watanabe, Z. He, and M. Kishi, "Measurement of Brillouin frequency shift distribution in PLC by Brillouin Optical Correlation Domain Analysis," Proc. of SPIE **8421,** 22nd International Conference on Optical Fiber Sensors (OFS-22), Beijing, China, paper 8421CE (2012).
23. R. Pant, C. G. Poulton, D. Y. Choi, H. Mcfarlane, S. Hile, E. Li, L. Thevenaz, B. Luther-Davies, S. J. Madden, and B. J. Eggleton, "On-chip stimulated Brillouin scattering," Opt. Express **19**(9), 8285–8290 (2011).
24. S. Levy, V. Lyubin, M. Klebanov, J. Scheuer, and A. Zadok, "Stimulated Brillouin scattering amplification in centimeter-long directly written chalcogenide waveguides," Opt. Lett. **37**(24), 5112–5114 (2012).

1. Introduction

Stimulated Brillouin scattering (SBS) in optical fibers is a nonlinear interaction between a relatively intense pump wave and a weaker, counter-propagating signal wave, which are coupled by a stimulated acoustic field [1]. Effective coupling requires that the difference between the optical frequencies of pump and signal matches the *Brillouin frequency shift* of the fiber ν_B ~10-11 GHz. Precise frequency matching is necessary, as the linewidth of the process for continuous pump waves is only about 30 MHz. Since the value of ν_B at a given fiber location varies with temperature and strain, the mapping of SBS interactions has been employed in the distributed sensing of both quantities for 25 years [2,3]. The most widely used measurement configuration is Brillouin optical time domain analysis (or B-OTDA), in which continuous signal waves are amplified by pump pulses, and the power of the output signal is observed as a function of time [3,4]. B-OTDA can reach 100 km range [5,6], and provide dynamic measurements [7], however the spatial resolution of the basic setup is restricted to the order of 1 m by the relatively long acoustic lifetime τ of about 5 ns [8]. Numerous methods were proposed to improve B-OTDA resolution (see a recent review in [9] and references therein). A resolution of 2 cm has been achieved along 2 km of fiber [10].

The magnitude of the stimulated acoustic wave at a given fiber location is given by the inner product between the complex envelopes of pump and signal at that point, weighted over an exponential window of duration 2τ [11]. Therefore, the spatial profile of the acoustic wave is closely related to the temporal cross-correlation between the two counter-propagating optical complex envelopes [12]. This property is at the basis of Brillouin optical correlation domain analysis (B-OCDA), proposed initially by Hotate and coauthors 15 years ago [13]. In B-OCDA, continuous-amplitude pump and signal waves are judiciously modulated, in

#206802 - $15.00 USD Received 19 Feb 2014; revised 28 Mar 2014; accepted 28 Mar 2014; published 12 May 2014
(C) 2014 OSA

frequency or phase, so that the cross-correlation between their complex envelopes is restricted to discrete and narrow peaks [13,14]. Frequency modulation-based B-OCDA reached a spatial resolution of 1.6 mm [15]. The range of unambiguous measurements in the basic configuration was restricted to hundreds of resolution points, due to the generation of multiple, periodic correlation peaks. The measurement range was later extended through more elaborate frequency modulation patterns [14]. Recent advances in B-OCDA include phase modulation by long, binary sequences for an extended measurement range [16]; time gating for improved signal-to-noise ratios (SNRs) [14,17]; use of special phase codes for reduced off-peak residual interactions and improved SNR [18]; and the combination between B-OTDA and B-OCDA for the simultaneous interrogation of a large number of peaks [18]. State-of-the-art B-OCDA setups provide few-km range alongside cm-scale resolution [17–19].

To the best of our knowledge, B-OCDA configurations reported to-date make use of broadband modulation of narrowband optical carriers. The further scaling of resolution in B-OCDA would require higher modulation rates, towards 100 GHz. External electro-optic modulators, millimeter-wave generators, or programmable pattern generators at these rates are seldom available. Alternatively, large-signal direct current modulation of laser diodes was successfully employed in frequency modulation B-OCDA [15]. A modulator at the output of the laser diode was required to compensate for the parasitic intensity variations that are associated with this scheme [15].

Herein, we propose and demonstrate for the first time a B-OCDA configuration which employs the broadband amplified spontaneous emission (ASE) of fiber amplifiers, rather than modulated carriers, as the common source of Brillouin pump and signal. The ASE source is split in two replicas: one serves as a pump wave, and the other is modulated in suppressed-carrier, double-sideband format by a sine wave of radio frequency $\nu \approx \nu_B$ and serves as a signal wave. The coherence length of the ASE source can be well below a millimeter and it does not depend on high-rate modulation. The single, narrow peak of cross-correlation between the pump and the signal is scanned along a fiber under test by a variable optical delay line.

ASE-based B-OCDA raises several challenges: first, the SBS power gain over millimeter-scale sections of standard silica fibers is very small. To make matters worse, unlike most B-OCDA setups, the intensity of the output signal wave is inherently fluctuating due to the stochastic nature of ASE [20]. Lastly, when the bandwidth of the source exceeds ν_B, the dual modulation side-bands in the signal wave are in spectral overlap. While one of these sidebands serves as a Brillouin Stokes wave, the other represents an anti-Stokes wave. The separation between Brillouin gain and loss at the signal output requires careful considerations. These issues are addressed in detail in the following sections.

Despite the inherent difficulties, we demonstrate below the reconstruction of the Brillouin gain spectra as a function of position along 5 cm of a silica single-mode fiber with a spatial resolution of 4 mm, using ASE-based B-OCDA. The scanning range was limited by the delay line available to us, and the restriction is not fundamental. The experimental uncertainty in the reconstruction of the local ν_B value is ± 1.5 MHz. A 4 mm-long hot spot is properly identified in the measurements. Preliminary results of this work have been briefly presented in [21]. The results establish a new potential approach to high-resolution Brillouin analysis, which might be particularly applicable to distributed Brillouin measurements along photonic devices [22–24].

#206802 - $15.00 USD Received 19 Feb 2014; revised 28 Mar 2014; accepted 28 Mar 2014; published 12 May 2014
(C) 2014 OSA

2. Principle of operation

2.1. Brillouin correlation domain analysis using broadband amplified spontaneous emission

The complex magnitude of the acoustic density variations in fiber position z and at time t is given by [11]:

$$Q(t,z) = jg_1 \int_0^t \exp\left[-\Gamma_A (t-t')\right] A_p\left(t' - \frac{z}{v_g}\right) A_s^*\left[t' - \frac{z}{v_g} + \theta(z)\right] \mathrm{d}t' \qquad (1)$$

In Eq. (1), g_1 is an electro-strictive parameter, v_g is the group velocity of light in the fiber, $A_p(t)$ denotes the instantaneous complex envelope of the SBS pump entering the fiber at $z = 0$ and propagating in the positive z direction, and $A_s(t)$ denotes the complex envelope of the counter-propagating signal wave which enters the fiber at $z = L$. The position-dependent temporal offset $\theta(z)$ is defined as: $\theta(z) \equiv (2z - L)/v_g$. Lastly, the bandwidth Γ_A is given by the angular frequency offset $\Omega = 2\pi\nu$ between the central optical frequencies of pump and signal, and the local value of the Brillouin shift $\Omega_B(z) = 2\pi\nu_B(z)$: $\Gamma_A(\nu, z) \equiv j\left[\left(\Omega_B^2(z) - \Omega^2 - j\Omega\Gamma_B\right)/2\Omega\right]$. It reduces to half the Brillouin linewidth $\Gamma_A = \frac{1}{2}\Gamma_B = 1/(2\tau)$ when $\nu = \nu_B(z)$.

In B-OCDA setups, the pump and signal waves are drawn from a single source and subsequently offset in frequency, so that $A_p(t) = A_{p0}u(t)$ and $A_s(t) = A_{s0}u(t)$. Here $u(t)$ is a common, normalized envelope function with an average magnitude of unity, and A_{p0} and A_{s0} are constants representing the average magnitudes of the pump and signal, respectively. In most measurement configurations reported to-date, $u(t)$ represents the deterministic frequency or phase modulation of a narrowband optical carrier. In contrast, herein $u(t)$ denotes the complex envelope of polarized thermal light from an ASE source of bandwidth $\Delta\nu^{in}$ and coherence time $\tau_c^{in} \approx 1/\Delta\nu^{in}$ [20].

The expectation value of the acoustic field magnitude at position z, for $t >> \tau$, is given by:

$$\begin{aligned}\overline{Q(z)} &= jg_1 A_{p0} A_{s0}^* \int_0^t \exp\left[-\Gamma_A (t-t')\right] \overline{u\left(t' - \frac{z}{v_g}\right) u^*\left[t' - \frac{z}{v_g} + \theta(z)\right]}\, \mathrm{d}t' \\ &= jg_1 A_{p0} A_{s0}^* \int_0^t \exp\left[-\Gamma_A (t-t')\right] \gamma_u\left[\theta(z)\right] \mathrm{d}t' = j\frac{g_1 A_{p0} A_{s0}^*}{\Gamma_A(\nu, z)} \gamma_u\left[\theta(z)\right] \qquad (2)\end{aligned}$$

In Eq. (2), $\gamma_u(\theta)$ denotes the auto-correlation of $u(t)$, an overhanging bar sign represents the ensemble average, and it has been assumed that the output of the ASE source can be described in terms of an ergodic random process [20]. We may therefore expect that the acoustic field would be confined to a single short segment, whose extent $\Delta z \approx \frac{1}{2} v_g \tau_c^{in}$ is given by half the correlation length of the source, located at the center of the fiber where $\theta\left(\frac{1}{2}L\right) = 0$ [11,16]. The position of the correlation peak can be scanned through a variable delay in the paths leading either the pump or the signal waves into the fiber under test [11,16].

Figure 1 shows an example of the numerical integration of Eq. (1), with both pump and signal drawn from a specific realization of polarized thermal light with a bandwidth of 25 GHz. The Brillouin frequency shift ν_B was constant along the simulated fiber section, and the

#206802 - $15.00 USD Received 19 Feb 2014; revised 28 Mar 2014; accepted 28 Mar 2014; published 12 May 2014
(C) 2014 OSA

frequency offset ν was chosen to match that value. The acoustic field is confined to a single and narrow correlation peak of 4 mm width, as anticipated. The results are analogous to those obtained with phase-coded B-OCDA [11,16], in which the spatial resolution Δz is determined by the spatial extent of a single coding symbol. The realization of shorter coherence times is technically much simpler than that of ultra-high-rate modulation by carefully designed sequences, as in [12,18].

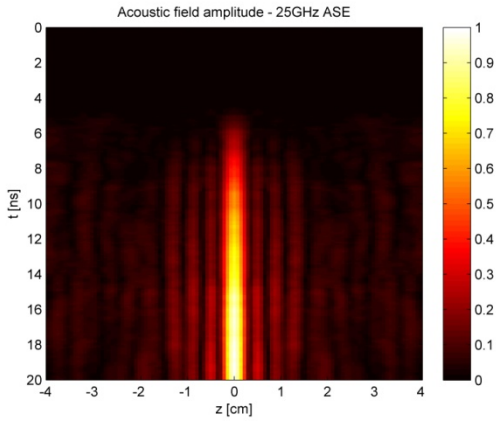

Fig. 1. Simulated magnitude of the acoustic wave density fluctuations (in normalized units), as a function of position and time along a 8 cm-long fiber section. Both pump and signal waves are drawn from a polarized amplified spontaneous emission source, filtered to a bandwidth of 25 GHz. The acoustic field, and hence the SBS interaction between pump and signal, is confined to a single correlation peak, whose spatial extent of 4 mm corresponds to half the coherence length of the filtered source.

In our experiments, the signal wave is generated through the suppressed-carrier, double-sideband modulation of the ASE source by a sine-wave of radio-frequency ν. Since $\Delta\nu^{in} >> \nu$, the two modulation sidebands are in spectral overlap. Most spectral components of the signal wave are therefore subject to both SBS amplification and attenuation. The problem could be alleviated using a single-sideband modulator; however one is not available to us. In order to overcome this inherent difficulty, an optical bandpass filter of bandwidth $\Delta\nu^{out} < \Delta\nu^{in}$ is placed at the output signal path, prior to detection. The central transmission frequency of the filter is tuned to the lower-frequency extremity of the signal spectrum. Hence the selected signal components are those that predominantly undergo SBS amplification along the fiber under test.

Note that the generation of a stationary acoustic field is stimulated by the unfiltered input signal wave, and hence governed by τ_c^{in} (see the simulated Fig. 1). Therefore, the SBS amplification of the entire signal wave can only take place when ν matches ν_B within that short segment. The filtering of the signal at the output, after the Brillouin interaction had already taken place, does not affect the spatial resolution. To further illustrate this point, we simulated the signal gain as a function of frequency offset and path imbalance between pump and signal, using direct integration of Eq. (1). The value of ν_B was locally offset by 40 MHz from its reference value within a 4 mm-long segment only. At the output of the fiber under test, the 25 GHz-wide signal wave was filtered to a bandwidth $\Delta\nu^{out}$ of 9 GHz. The gain map shown in Fig. 2 illustrates a spatial resolution of 4 mm, which corresponds to τ_c^{in} as discussed above. The map is practically indistinguishable from that obtained without an output filter.

#206802 - $15.00 USD Received 19 Feb 2014; revised 28 Mar 2014; accepted 28 Mar 2014; published 12 May 2014
(C) 2014 OSA

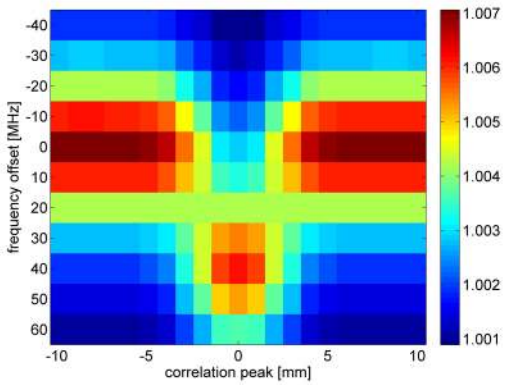

Fig. 2. Simulated stimulated Brillouin scattering power amplification of a signal wave, as a function of the frequency offset between the central frequencies of the pump and signal waves and the position of their correlation peak along 20 millimeters of a fiber under test. The Brillouin shift of the fiber at room temperature is taken as zero frequency. The Brillouin shift within a 4 millimeter-long segment at the center of the fiber under test was raised by 40 MHz. Both pump and signal waves are drawn from a 25 GHz-wide polarized amplified spontaneous emission source. The signal wave at the output of the fiber under test was filtered to a bandwidth of 9 GHz prior to detection. The simulation indicates a spatial resolution of 4 mm, which corresponds to half the coherence length of the input, 25 GHz-wide signal.

2.2. Signal-to-noise ratio analysis

Consider first the measurement of an output signal wave that is unaffected by SBS, using a photo-detector with an integration time T. The detector output is proportional to the quantity:

$$W(t) \equiv \left|A_{s0}\right|^2 \int_{t-T}^{t} \left| u\left(t' - \frac{L}{v_g}\right)\right|^2 dt' \tag{3}$$

As the signal wave is drawn from an ASE source, $W(t)$ is a random process. The expectation value of the photo-detector output is $\bar{W} = \left|A_{s0}\right|^2 T$ [20]. Since the process is assumed to be ergodic, the time dependence in $\bar{W}$ is dropped. Assuming that T is much longer than the coherence time of the filtered output signal wave $\tau_c^{out} \approx 1/\Delta\nu^{out}$, the standard deviation of the detector reading can be approximated as $\sigma_W \approx \bar{W}\sqrt{\tau_c^{out}/T}$ [20]. The expected increment in $\bar{W}$ due to SBS amplification with $\nu = \nu_B$ is given by: $\Delta W = \bar{W}\left[\exp\left(g_0\left|A_{p0}\right|^2 \cdot \Delta z\right) - 1\right] \approx \bar{W} \cdot g_0\left|A_{p0}\right|^2 \cdot \Delta z$, where g_0 (in units of [W·m]$^{-1}$) is the SBS gain coefficient of the fiber under test. The SNR of the SBS amplification measurement can therefore be estimated as:

$$\mathrm{SNR} \equiv \frac{\Delta W}{\sigma_W} \approx g_0\left|A_{p0}\right|^2 \cdot \Delta z\sqrt{\frac{T}{\tau_c^{out}}} \approx \frac{1}{2} g_0 v_g \frac{\left|A_{p0}\right|^2}{\Delta\nu^{in}}\sqrt{\frac{\Delta\nu^{out}}{B}} \tag{4}$$

Here $B \approx 1/T$ is the integration bandwidth of the photo-detector, and the output signal power is assumed to be sufficiently high to overcome the detector thermal noise. The SNR scales with the power spectral density of the pump wave, and with the square root of the ratio between the output signal bandwidth and the detector bandwidth. In our experiments $\Delta\nu^{in}$ is approximately 25 GHz, $\Delta\nu^{out}$ is about 9 GHz, B equals 200 MHz, $\left|A_{p0}\right|^2$ is on the order of

#206802 - $15.00 USD Received 19 Feb 2014; revised 28 Mar 2014; accepted 28 Mar 2014; published 12 May 2014
(C) 2014 OSA

10 W, and g_0 is estimated as 0.2 $[\mathrm{W{\cdot}m}]^{-1}$. The expected SNR of a single acquisition trace is very low, on the order of 0.05. Averaging over a large number of repeating measurements is therefore necessary. The SNR estimate of Eq. (4) is supported by numerical simulations of SBS interactions driven by ASE sources, such as that leading to Fig. 1, using a range of $\Delta\nu^{in}$ and $\Delta\nu^{out}$ values. The calculated SNRs are within 1 dB of the corresponding predictions. The simulations also verify the functional dependence of the SNR on $\Delta\nu^{in}$, $\Delta\nu^{out}$ and B.

3. Experimental setup and results

Figure 3 shows the experimental setup used in high resolution B-OCDA measurements based on an ASE source [21]. Light from an erbium-doped fiber amplifier (EDFA), operating with its input disconnected, passed through a fiber-optic polarization beam splitter and a tunable optical band-pass filter of 25 GHz bandwidth. The source bandwidth corresponds to an expected spatial resolution Δz of 4 mm. The filtered, polarized ASE source was split in two paths by a fiber-optic coupler. Light in the pump branch was amplitude-modulated by pulses of 25 ns duration and 2 μs period, amplified to an average power of 200 mW (peak power of approximately 10 W), and launched into one end of a 2 m-long fiber under test via a circulator. The fiber under test was a silica single-mode fiber with a relatively small mode field diameter of 6.7 μm.

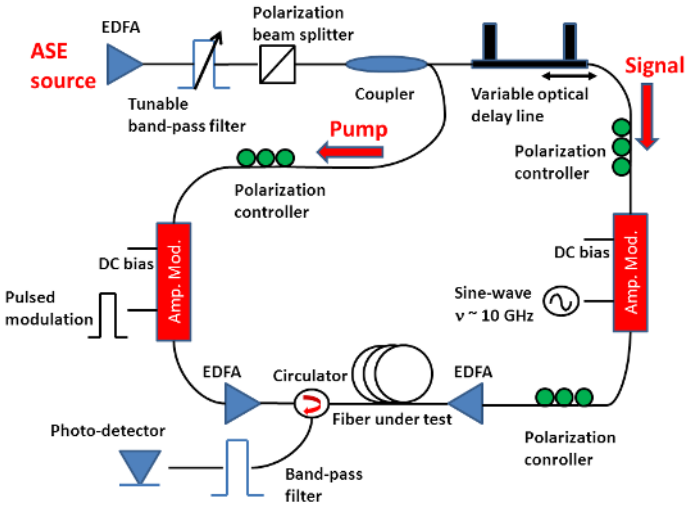

Fig. 3. Experimental setup for Brillouin optical correlation domain analysis using a broadband amplified spontaneous emission (ASE) source. EDFA: erbium-doped fiber amplifier. Amp. Mod.: amplitude modulator [21].

Light in the signal path was modulated in suppress-carrier, double-sideband format by an electro-optic amplitude modulator, driven by a sine wave of radio frequency ν. The signal wave was transmitted through a manually-variable optical delay line, amplified to an average power of 10 mW, and launched into the opposite end of the fiber under test. The signal wave at the fiber under test output passed through the fiber-optic circulator and a 9 GHz-wide optical band-pass filter, which retained only part of the low-frequency spectral contents of the dual-sideband signal wave. Figure 4 shows the optical power spectra of the pump wave, the input signal wave and the output signal wave. The filtered output signal was detected by a photo-receiver of 200 MHz bandwidth, and sampled by a real-time digitizing oscilloscope.

#206802 - $15.00 USD Received 19 Feb 2014; revised 28 Mar 2014; accepted 28 Mar 2014; published 12 May 2014
(C) 2014 OSA

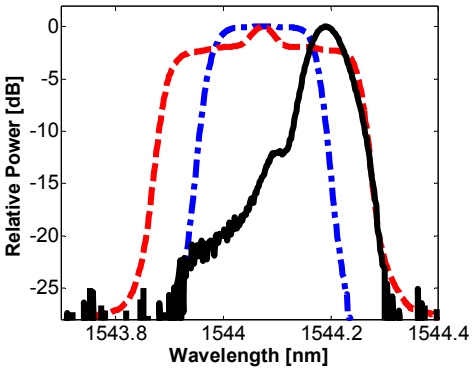

Fig. 4. Normalized optical power spectral densities of the pump wave (blue, dash-dotted), input signal wave (red, dashed), and filtered output signal wave (black, solid).

The lengths of fibers in the signal and pump branches were matched so that the single correlation peak between the two waves fell within the fiber under test. The position of the correlation peak could be scanned over a range of 5 cm by the manual variable delay line. The output signal was recorded for a range of modulation frequencies ν in the vicinity of the Brillouin shift ν_B of the fiber under test, and for a range of manual position variations in 2.5 mm increments. The SNR of a single acquisition trace was as low as 0.1, in general agreement with the predictions of section 2.2. Hence each trace was averaged over 4,096 repetitions. A 4 mm-long section of the fiber under test, located within the scanning range, was heated locally to 55 °C.

Figure 5(a) presents the relative measured SBS amplification of the signal $\Delta W(\nu, z)$. The local SBS gain spectra are centered at ν_B ~10.2 GHz at room temperature, and characterized by a full width at half maximum of approximately 30 MHz, in agreement with expectations. Figure 5(b) shows $\nu_B(z)$, estimated by Lorentzian fitting of the experimental gain spectra. The local hot spot is properly identified. For comparison, $\nu_B(z)$ is also shown for a measurement in which the hot spot was removed. The standard deviation in the reconstructed $\nu_B(z)$ is ± 1.5 MHz.

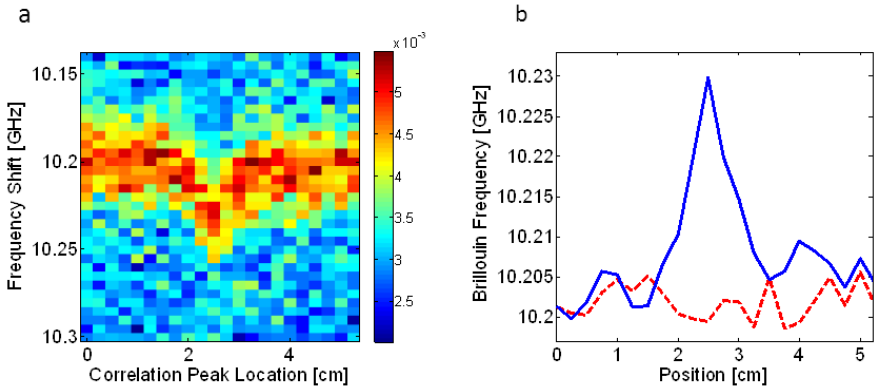

Fig. 5. (a) Measured peak voltage of the output signal wave, as a function of the frequency offset between pump and signal and the manual position offset of the correlation peak location. A 4 mm-long hot spot was introduced near the center of the scanning range. (b) Reconstructed local Brillouin frequency shift as a function of position, with the hot spot turned on (blue, solid) and off (red, dashed).

#206802 - $15.00 USD Received 19 Feb 2014; revised 28 Mar 2014; accepted 28 Mar 2014; published 12 May 2014
(C) 2014 OSA

4. Summary

A novel B-OCDA technique was proposed and demonstrated based on the ASE of an EDFA. The method employs for the first time a source of physical noise, rather than modulated carriers, in the generation of broadband Brillouin pump and signal waves. In a proof-of-concept experiment, measurements were performed over 5 cm of fiber with a spatial resolution of 4 mm. A 4 mm-long localized hot spot within the measurement range was properly recognized. This new approach takes advantage of simple optical noise, instead of high-end electronic devices, to obtain high resolution. A stable localized SBS interaction could be achieved using fluctuating optical fields. The spatial resolution of the proposed method is scalable towards 1 mm and less, beyond those of phase-coded B-OCDA schemes. Sections of highly-nonlinear fibers may be used to enhance the Brillouin amplification over such short segments.

The measurement SNR is fundamentally restricted by fluctuations due to the stochastic nature of ASE [20]. The experimental SNR of a single acquisition trace was as low as 0.1, in general agreement with predictions. Averaging over 4,096 repeating measurements was therefore employed. The SNR is inferior to those of other high-resolution Brillouin analysis schemes, such as phase-coded and frequency-coded B-OCDA [17–19] or high-resolution B-OTDA [9,10], in which the magnitude of the signal wave is, at least in principle, deterministic. These systems can be designed to be limited by detector thermal noise. Another difficulty associated with the reported experiment is the limited range and inconvenience of manual position scanning. Motorized delay lines providing longer scanning ranges are readily available. The number of resolution points could reach several hundreds.

In conclusion, the new form of B-OCDA could provide distributed Brillouin sensing in greater detail over short segments, for example within photonic devices [22–24].

Acknowledgment

This work was supported in part by the Chief Scientist Office, the Israeli Ministry of Industry, Trade and Labor, through the KAMIN program.